A new approach to quantitative azimuthal inversion for stress and fracture detection.

Peter Mesdag, CGG

Summary

A method is described to allow quantitative usage of isotropic modeling and inversion in anisotropic media. Based on the Rüger reflectivity equations for HTI media, transforms are designed for the elastic parameters used in pre-stack inversion. The transformed elastic parameters can be used in isotropic forward modeling and inversion to accurately mimic the anisotropic reflectivity behavior of the seismic data. The proposed method allows us to close the loop between well log data and seismic inversion results using existing isotropic forward modeling and inversion tools.

In this paper a synthetic feasibility study will be shown, indicating that we can exactly predict the outcome of a wide azimuth (WAZ) seismic inversion experiment based on isotropic elastic parameters and Thomsen's anisotropy parameters for HTI media.

The technique has been successfully applied to several real data sets. (Zhang and Mesdag, 2016).

Introduction

Connolly (1999) introduced the concept of Elastic Impedance (EI) and related concepts Extended Elastic Impedance and Gradient Impedance (EEI, GI). These non-physical elastic parameters allowed us to use post-stack inversion algorithms to do quantitative analysis on pre-stack or partial stack seismic data.

Since that time, technology has evolved and pre-stack simultaneous inversion has become industry standard. It has also been extended to simultaneous azimuthal inversion (e.g. Downton and Roure, 2010). In full anisotropic azimuthal inversion, the extra dimensionality of the solution space needs to be reduced to be able to find a stable solution. This is usually achieved by assuming underlying fracture models.

In this paper we introduce a different approach to inversion in anisotropic media. We define elastic parameter transforms that allow us to use pre-stack isotropic modeling and inversion in anisotropic media. These parameter transforms are based on the Rüger equations for VTI and HTI media. The transformed elastic parameters allow us to use our regular workflows to calibrate and invert seismic data using our standard tools and pre-stack inversion techniques.

After inversion, the azimuthal bias in the elastic parameters takes on a particular form which can be analyzed using our knowledge of the transforms. The way we analyze the elastic volumes will also be described here.

Method

For weak anisotropy and an isotropic half space overlying a HTI medium, Rüger (1998) defined a P-wave reflectivity expression. This equation contains the isotropic elastic parameters and three Thomsen parameters representative of the HTI-medium and is a function of the angle of incidence and the anisotropy plane orientation (the azimuth of the anisotropy).

$$R_p(\theta) = R_0 + R_2 \sin^2\theta + R_4 \sin^2\theta \tan^2\theta \qquad (1)$$

where

$$R_0 = \frac{1}{2}\frac{\Delta Z_p}{\overline{Z}_p}$$

$$R_2 = \frac{1}{2}\left[\frac{\Delta V_p}{\overline{V}_p} - \left(\frac{2\overline{V}_s}{\overline{V}_p}\right)^2 \frac{\Delta G}{\overline{G}} + \left\{\Delta\delta^{(v)} + 8\left(\frac{\overline{V}_s}{\overline{V}_p}\right)^2 \Delta\gamma\right\}\cos^2(\omega-\phi)\right]$$

$$R_4 = \frac{1}{2}\left[\frac{\Delta V_p}{\overline{V}_p} + \Delta\epsilon^{(v)}\cos^4(\omega-\phi) + \Delta\delta^{(v)}\sin^2(\omega-\phi)\cos^2(\omega-\phi)\right]$$

By manipulating this reflectivity expression further, the isotropic parameters can be recast into three effective elastic parameters. These can be used in isotropic modeling to create close approximations to anisotropic reflectivity and they can be used in an isotropic pre-stack inversion scheme. The transforms from anisotropic parameters to pseudo-isotropic parameters are as follows:

$$V_P' = \left[\delta_r^{(V)}\right]^{\cos^2(\phi-\omega)} \left(\frac{\varepsilon_r^{(V)}}{\delta_r^{(V)}}\right)^{\cos^4(\phi-\omega)} V_P, \qquad (2)$$

$$V_S' = \left(\frac{\sqrt{\delta_r^{(V)}}}{\gamma_r^{(V)}}\right)^{\cos^2(\phi-\omega)} \left(\frac{\varepsilon_r^{(V)}}{\delta_r^{(V)}}\right)^{\frac{4K+1}{8K}\cos^4(\phi-\omega)} V_S, \qquad (3)$$

$$\rho' = \left[\delta_r^{(V)}\right]^{-\cos^2(\phi-\omega)} \left(\frac{\varepsilon_r^{(V)}}{\delta_r^{(V)}}\right)^{-\cos^4(\phi-\omega)} \rho. \qquad (4)$$

Where the ‘ indicates the pseudo or effective elastic parameter, Vp, Vs and ρ are the isotropic P-Velocity, S-Velocity and Density, respectively, and K is the average squared isotropic solid Vs/Vp ratio. The survey azimuth, and the anisotropy plane azimuth are given by ω and ϕ respectively. The Thomsen parameters $\varepsilon^{(v)}$, $\delta^{(v)}$ and $\gamma^{(v)}$ of the HTI medium (indicated by the superscript V are expressed as relative measures (indicated by the subscript r):

$$\varepsilon_r^{(V)} = \frac{\varepsilon^{(V)} + 1 - \overline{\varepsilon}^{(V)}}{1 - \overline{\varepsilon}^{(V)}}, \qquad (5)$$

$$\delta_r^{(V)} = \frac{\delta^{(V)} + 1 - \overline{\delta}^{(V)}}{1 - \overline{\delta}^{(V)}}, \qquad (6)$$

$$\gamma_r^{(V)} = \frac{\gamma^{(V)} + 1 - \overline{\gamma}^{(V)}}{1 - \overline{\gamma}^{(V)}}, \qquad (7)$$

where the over bars indicate average quantities. The pseudo-isotropic parameters given in Equations (2) – (4) degenerate into isotropic expressions when the survey azimuth is at right angles with the anisotropy plane azimuth, where $\phi - \omega = 90^\circ$. From Equations (2) – (4) follows that the pseudo-P-Impedance and pseudo Vp/Vs-ratio are given by:

$$I_P' = I_P, \qquad (8)$$

$$\left(\frac{V_P}{V_S}\right)' = \left[\sqrt{\delta_r^{(V)}\gamma_r^{(V)}}\right]^{\cos^2(\phi-\omega)} \left(\frac{\varepsilon_r^{(V)}}{\delta_r^{(V)}}\right)^{\frac{4K-1}{8K}\cos^4(\phi-\omega)} \frac{\overline{V_P}}{\overline{V_S}} \qquad (9)$$

The pseudo-P-Impedance is equal to the isotropic P-Impedance, which is consistent with the fact that azimuthal anisotropy effects manifest themselves on the far offsets only (Equation (1)).

Elastic Volumes Analysis

In the analysis of the azimuthally oriented elastic volumes we fit a trend to azimuthal variations in elastic properties. Its general expression for the natural logarithm of a pseudo-elastic parameter $\boldsymbol{A}'$ is:

$$A' = b_0 + b_1\cos[2(\phi-\omega)] + b_2\cos[4(\phi-\omega)] \qquad (10)$$

For instance for Vp/Vs the coefficients $b_0 - b_2$ follow form equation (9):

$$b_0 = \ln\frac{V_P}{V_S} + \frac{1}{2}\ln\gamma_r + \left(\frac{4K+3}{64K}\right)\ln\delta_r + \left(\frac{12K-3}{64K}\right)\ln\varepsilon_r$$

$$b_1 = \frac{1}{2}\ln\gamma_r + \frac{1}{16K}\ln\delta_r + \left(\frac{4K-1}{16K}\right)\ln\varepsilon_r$$

$$b_2 = -\left(\frac{4K-1}{64K}\right)\ln\delta_r + \left(\frac{4K-1}{64K}\right)\ln\varepsilon_r$$

By running the evaluation the three coefficients b_0, b_1, b_2 are output by an inversion process, as well as the orientation of the anisotropy plane ϕ and a statistical QC volume χ^2. The coefficients are related to the amplitude or strength of the anisotropy effect and the χ^2 QC is related to the goodness of fit for the model. In general the coefficient b_2 is significantly smaller than b_1. For instance b_2 vanishes if the Vp/Vs ≈ 2 or $\delta_r \approx \varepsilon_r$.
In the evaluation, a choice is made for the sign of b_1. Anisotropy axis orientation from seismic data suffers from a 90 degree ambiguity. In the most general case this ambiguity cannot be resolved without assuming a physically realistic underlying model. In the evaluation, the ambiguity is overcome by choosing a sign of b_1.
It can be shown that b_1 is negative for the inverted Vp/Vs parameter in HTI media under the Hudson dry crack model assumption (Hudson, 1980, Bakulin et al., 2000). In addition it can be shown that for the same HTI media b_1 is positive for the inverted Density parameter.

Feasibility

In this section we will go through a feasibility study, for which the steps are illustrated in Figure 1.

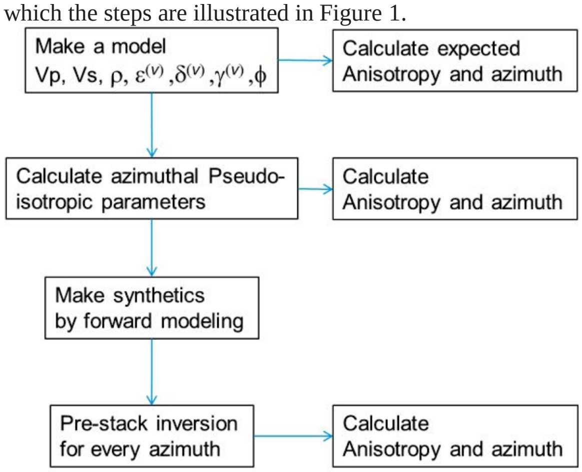

Figure 1: Workflow for an HTI feasibility study

We first make a notional model of the HTI anisotropic subsurface defined in isotropic elastic parameters, the three Thomsen parameters and the anisotropy axis orientation. Figure 2 shows a cross section of the isotropic elastic parameters, which were generated using simple geostatistical modeling based on real well log probability distributions.

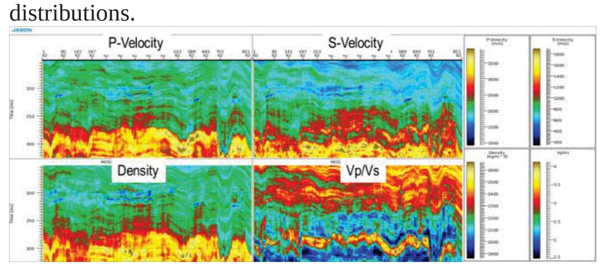

Figure 2: A cross section through the synthetic model, depicting the isotropic elastic parameters Vp, Vs, Rho and Vp/Vs.

Figure 3 shows a cross section through the Thomsen parameter and anisotropy azimuth volumes used in this experiment. Note that even though the anisotropy layers follow structure, their choice of magnitude and vertical position in the isotropic elastic model is arbitrary, i.e. there is no imposed physical relationship between the Thomsen parameters and the elastic parameters.
We will be choosing an inversion parameterization of Ip, Vp/Vs and Density. Knowing the relationships defined in the previous section, we can, from this model, directly calculate what we expect to come out of our inversion in terms of Vp/Vs and Density anisotropy (Figure 1, top right).

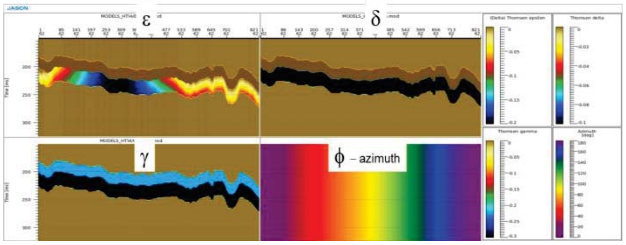

Figure 3: The same cross section through the model depicting the three Thomsen parameters and the anisotropy symmetry axis.

In Figure 4 the expected outcome of the experiment for b_1 in Equation 10 is shown for the parameters Vp/Vs and Density. Note that for this choice of elastic parameters and Thomsen parameters the Vp/Vs anisotropy is negative and the Density anisotropy is positive. I.e. The pseudo Vp/Vs is highest in the isotropic plane and lowest in the anisotropic plane. In HTI the isotropic plane is the vertical plane perpendicular to the anisotropy axis. The anisotropic plane is the vertical plane parallel to the anisotropy axis. For the pseudo density this is reversed, the pseudo density is highest in the anisotropy plane. This information will be used later in the analysis of the elastic volumes to choose the appropriate branch (sign of b_1).

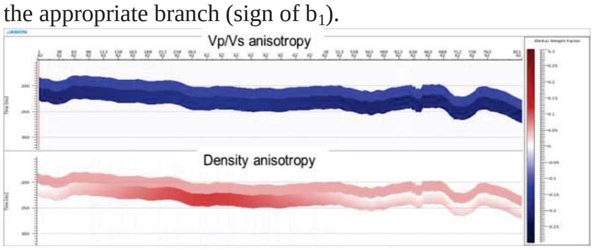

Figure 4: The expected anisotropy from an isotropic inversion experiment, given the parameters in Figures 2 and 3.

In a second step, we calculate the azimuthally oriented effective elastic parameters as described in equations (4) and (9). As Density is often not a viable independent parameter coming from limited offset seismic inversion we will concentrate on the Vp/Vs anisotropy and orientation.

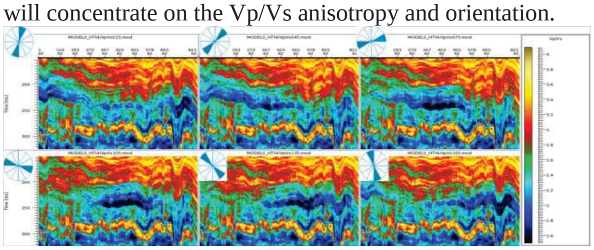

Figure 5: Azimuthally sectored pseudo Vp/Vs

To effectively describe the azimuthal behavior of the pseudo elastic parameters (Equation 10) we need at least 5 samples in the azimuthal direction. As shown in Figure 5 we have chosen 6 sectors for this experiment.

Now we will use the elastic volumes analysis to come up with estimates of the Vp/Vs anisotropy and the anisotropy symmetry axis orientation. Using the input shown in Figure 5, the outcome is shown in the lower panels of Figure 6. Note that there is no information loss and the analysis tool is doing its job well. Only where there is no anisotropy does the tool default to 0 (North or purple).

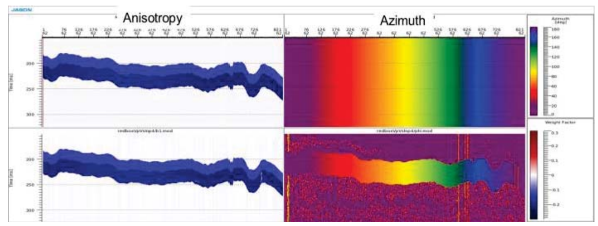

Figure 6: Expected anisotropy (top) and calculated anisotropy (bottom) from the azimuthally sectored pseudo Vp/Vs.

The next step in the feasibility workflow is calculation of the azimuthally-oriented pre-stack or partial stack seismic data. This forward modeling can be done by using the initial model and anisotropic forward modeling or by using the azimuthally oriented effective parameters and isotropic forward modeling. These two alternatives give exactly the same seismic synthetics, meaning that the assumptions used in our methodology are sufficiently accurate.

In a first pass, we used a real wavelet from a shallow seismic survey, which went up to 200 Hz (-6dB) had a low frequency cut-off around 16-20 Hz. We used 6 partial angle stacks ranging from 0 to 55 degrees. No noise was added to the synthetic seismic data.

The final step in the workflow is to invert every azimuth separately with a pre-stack inversion program. The inverted full bandwidth Vp/Vs and Density per azimuth are then input to the elastic volumes evaluation to yield estimates of b_0, b_1 and b_2 and the anisotropy symmetry axis orientation after inversion. The results for b_1 coming out of our experiment are compared with the expected values for the inverted Vp/Vs in Figure 7.

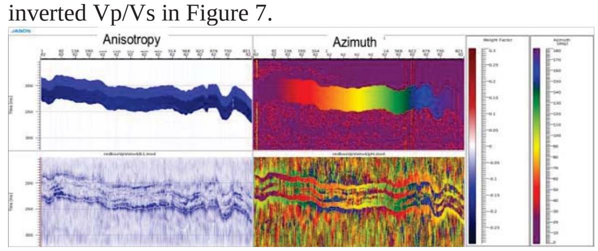

Figure 7: The expected Vp/Vs anisotropy (top) and calculated anisotropy after inversion.

Even though our individual sectored inversion are full bandwidth, the anisotropy only shows up at the interfaces where the anisotropy changes. Also the azimuth shows 90 degree ambiguity in many places.
After some thought, the reason for this was found. The seismic data fundamentally is lacking the low frequencies and we are using the same isotropic trend model for every one of our azimuthally sectored inversions. So the low frequency component is lacking azimuthal variation and the anisotropy estimates are missing the low frequency information.
This can be simply verified by filtering off the lower frequencies from our expected anisotropy in the top left panel of Figure 7. If we use a 20Hz cut off as suggested by the wavelet we used, the result is shown in Figure 8. Now we clearly see the similarities between the upper and the lower panels of the anisotropy. Moreover, where we have chosen the incorrect branch in the analysis, i.e. where we see the side lobes of the band limited data, we are mis-interpreting the azimuth by 90 degrees.

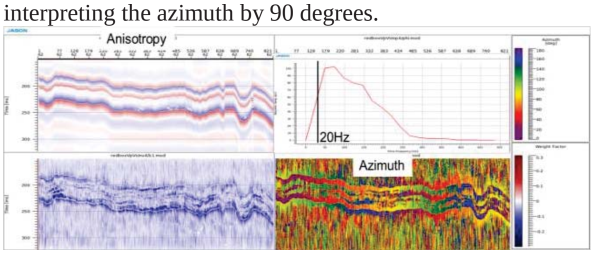

Figure 8: As Figure 7, but comparing with the initial model after the application of the low frequency cut off (top left) of the wavelet (top right).

With this knowledge from the first pass we re-did the seismic synthetic generation and the inversion, but now with a broadband wavelet with a low frequency cut off of around 6Hz.
The final result from the inversion and analysis is shown in Figure 9. Even though we are still lacking the lower 6 Hz of the anisotropy information, we see that the analysis results much better predict our expected anisotropy distribution.

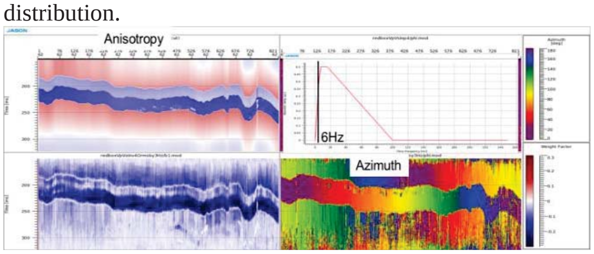

Figure 9: As Figure 8, using a broadband wavelet in the experiment and with a 6Hz low frequency cut off in the upper left panel.

Conclusions

We have developed a method to quickly test inversion sensitivity under anisotropic conditions. We use effective input models and isotropic modeling and inversion.
The azimuthal low frequency model is unknown in a first iteration, so we need to use expected low frequency cut off in analysis.
In the analysis of final inversions a branch is chosen. This results in a polarity reversal where the inversion produces side lobes. A polarity reversal results in a 90^0 azimuth shift in the analysis.
As the azimuthal information is not known before hand away from well control you preferably need broadband seismic to recover the low frequencies.

Acknowledgement

I would like to thank my colleagues Raphael Bornard and Harry Debeye who helped develop the theory and Leonardo Quevedo for developing the evaluation tool.

EDITED REFERENCES

Note: This reference list is a copyedited version of the reference list submitted by the author. Reference lists for the 2016 SEG Technical Program Expanded Abstracts have been copyedited so that references provided with the online metadata for each paper will achieve a high degree of linking to cited sources that appear on the Web.

REFERENCES

Bakulin, A., V. Grechka, and I. Tsvankin, 2000, Estimation of fracture parameters from reflection seismic data part I HTI model due to single fracture set: Geophysics, **65**, 1788–1802, http://dx.doi.org/10.1190/1.1444863.

Connolly, P., 1999, Elastic impedance: The Leading Edge, **18**, 438–452, http://dx.doi.org/10.1190/1.1438307.

Downton, J., and B. Roure, 2010, Azimuthal simultaneous elastic inversion for fracture detection: 80th Annual International Meeting, SEG, Expanded Abstracts, 263-267, http://dx.doi.org/10.1190/1.3513389.

Hudson, J. A., 1980, Overall properties of a cracked solid: Mathematical Proceedings of the Cambridge Philosophical Society, **88**, 371–384, http://dx.doi.org/10.1017/S0305004100057674.

Rüger, A., 1998, Variation of P-wave reflectivity with offset and azimuth in anisotropic media: Geophysics, **63**, 935–947, http://dx.doi.org/10.1190/1.1444405.

Zhang and Mesdag, personal communication, 2016.